On the Combustion of Terpenes Biofuels and Pollutants Characterization Through High-Resolution Mass Spectrometry

Philippe Dagaut, Zahraa Dbouk, Roland Benoit

Proceedings of ASME Turbo Expo 2024
Turbomachinery Technical Conference and Exposition
GT2024
June 24-28, 2024, London, United Kingdom

GT2024-121549

ON THE COMBUSTION OF TERPENES BIOFUELS AND POLLUTANTS CHARACTERIZATION THROUGH HIGH-RESOLUTION MASS SPECTROMETRY

Philippe Dagaut[1], Zahraa Dbouk[1], Roland Benoit[1]

[1]CNRS-INSIS, ICARE, 1C Ave. Recherche Scientifique, 45071 Orleans, France

ABSTRACT

Terpenes are a class of hydrocarbon compounds naturally found in plants. They already have a variety of uses, such as flavor and fragrance additives. Also, they can be blended with conventional or synthetic liquid fuels. Understanding the kinetics of terpenes combustion is important for the development of cleaner combustion, as well as for evaluating associated air pollution and environmental impacts. Therefore, the oxidation of terpenes has been performed under well-controlled conditions. The cool flame oxidation of limonene, α-pinene, and β-pinene, terpenes commonly emitted by vegetation, was performed in a jet-stirred reactor under fuel-lean conditions, at 1 bar. Samples of the reacting mixtures were collected, dissolved in acetonitrile, and analyzed by high-resolution mass spectrometry. Direct flow injection and chromatographic separation by ultra-high-performance liquid chromatography were used. Heated electrospray ionization and atmospheric pressure chemical ionization were employed to characterize the products of oxidation. H/D exchange using D_2O was performed for probing the presence of hydroxyl and hydroperoxyl groups in the products. The Brady reaction was used to assess the presence of carbonyl functional groups in the products. A large set of oxidation products, including highly oxidized organic products with 5 and more oxygen atoms, was observed. Besides, FTIR analyzes of gas products were performed. Aromatic and/or polyunsaturated products were detected. Graphic tools including Van Krevelen plots, aromaticity index, and maximum carbonyl ratio, and Venn plots were used to analyze the results. Reaction pathways are proposed to rationalize the results.

Keywords: Biofuel, Terpenes, Pollutants, Orbitrap

NOMENCLATURE

φ	equivalence ratio
2,4-DNPH	2,4-dinitrophenylhydrazine
ACN	acetonitrile
AI	aromaticity index
APCI	atmospheric pressure chemical ionization
BDE	bond dissociation energy
CF	cool-flame
DBE	double bond equivalent
FIA	flow injection analysis
HCD	higher-energy collision dissociation
HESI	heated electrospray ionization
HPLC	high-pressure liquid chromatography
HRMS	high-resolution mass spectrometry
JSR	jet-stirred reactor
KHP	ketohydroperoxide
MCR	maximum carbonyl ratio
MS	mass spectrometry
RH	hydrocarbon
RP-UHPLC	reverse-phase ultra-high-performance liquid chromatography
VK	Van Krevelen
VOCs	volatile organic compounds

1. INTRODUCTION

Terpenes pertain to a chemical class of hydrocarbons produced by vegetation and naturally released into the troposphere. They represent a large portion of volatile organic chemicals (VOCs) present in the troposphere [1]. Also, due to their high-energy-density, they represent interesting liquid biofuel candidates to reduce transportation carbon footprint [2, 3]. Cetane numbers of ~20 have been reported which make them usable as drop-in fuel for ground and air transportation. Blends composition would need to meet fuel standards which depend on applications (ground or air). But their introduction as biofuel or drop-in fuel would most likely increase their emission in the troposphere. Emissions of unburnt fuel, and evaporation during fuel processing and refueling would contribute. The kinetics of oxidation of terpenes under tropospheric conditions has received much attention, as reported earlier [4, 5]. Nevertheless, the knowledge of the oxidation pathways involved has not been fully unveiled [5-8]. Until recently, the characterization of the chemical kinetics of combustion of this class of hydrocarbons has not received much attention [4, 5, 9]. Indeed, only burning velocities in air, flame structures, and effect of terpenes on

ignition had been reported in the literature [10-14]. Whereas at high temperature, the combustion of hydrocarbons (RH) is relatively well understood, in the CF regime, it produces a large set of oxygenated products and reaction pathways are still discussed. Among the products, ketohydroperoxides (KHPs) produced through a sequence of chemical reactions [15, 16] are recognized for being responsible for chain branching under CF conditions (Figure 1).

$$RH + {}^{\bullet}OH \rightarrow R^{\bullet} + H_2O \quad (1)$$
$$R^{\bullet} + O_2 \rightleftarrows ROO^{\bullet} \quad (2)$$
$$ROO^{\bullet} + HOO^{\bullet} \rightleftarrows ROOH + O_2 \quad (3)$$
$$ROO^{\bullet} + RH \rightleftarrows ROOH + R^{\bullet} \quad (4)$$
$$ROO^{\bullet} \rightleftarrows {}^{\bullet}QOOH \quad (5)$$
$$ROO^{\bullet} \rightleftarrows Q \text{ (unsaturated product)} + HOO^{\bullet} \quad (6)$$
$${}^{\bullet}QOOH \rightleftarrows {}^{\bullet}OH + QO \text{ (cyclic ether)} \quad (7)$$
$${}^{\bullet}QOOH + O_2 \rightleftarrows {}^{\bullet}OOQOOH \quad (8)$$
$${}^{\bullet}OOQOOH \rightleftarrows HOO^{\bullet}Q'OOH \quad 9)$$
$$HOO^{\bullet}Q'OOH \rightleftarrows {}^{\bullet}OH + HOOQ'{=}O \text{ (KHPs)} \quad (10)$$
$$HOOQ'{=}O \rightleftarrows {}^{\bullet}OH + OQ''O \quad (11)$$

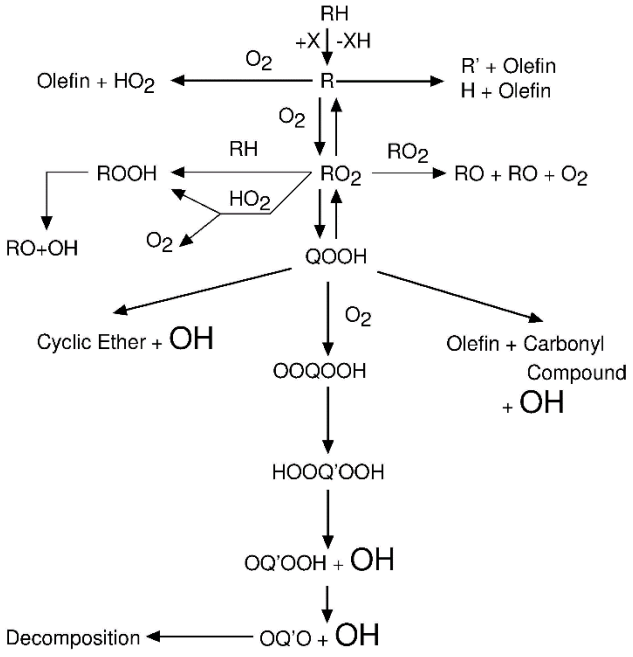

FIGURE 1: Simplified oxidation scheme for hydrocarbons.

In the recent years, the formation of more oxygenated products in CF was observed for a wide range of fuels including hydrocarbons and oxygenated compounds [4, 5, 9, 17-20]. These products are formed via alternative oxidation routes which involve an internal H-transfer in ˙OOQOOH radicals. This H-transfer occurs on another H–C group rather than on the H–COOH group which is responsible for KHPs formation (Reactions 9 and 10). Then, it opens new oxidation pathways including at least a third O_2 addition to HOO˙Q'OOH yielding ˙OOQ'$(OOH)_2$. This sequence of reactions, i.e., H-transfer and O_2 addition can occur several times, yielding highly oxidized products [19, 21-23].

$$HOO^{\bullet}Q'OOH + O_2 \rightarrow {}^{\bullet}OOQ'(OOH)_2 \quad (12)$$
$${}^{\bullet}OOQ'(OOH)_2 \rightarrow HOO^{\bullet}Q''(OOH)_2 \rightarrow O{=}Q'(OOH)_2 + OH \quad (13)$$

˙QOOH radicals can decompose yielding stable products and radicals via Reactions (7), (14), and (15).

$${}^{\bullet}QOOH \rightarrow \text{olefin} + \text{carbonyl} + {}^{\bullet}OH \quad (14)$$
$${}^{\bullet}QOOH \rightarrow HOO^{\bullet} + \text{olefin} \quad (15)$$

For unsaturated hydrocarbons, including terpenes, oxidation via the Waddington mechanism [24] can occur. The reaction starts by ˙OH addition on a C=C double bond followed by O_2 addition and internal H-atom transfer from the –OH group to the –OO˙ peroxy group, followed by decomposition:

$$R{-}C{=}C{-}R' + {}^{\bullet}OH \rightleftarrows R{-}{}^{\bullet}C{-}C(-R')-OH \quad (16)$$
$${}^{\bullet}C(-R)-C(-R')-OH + O_2 \rightleftarrows {}^{\bullet}OO-C(-R)-C(-R')-OH \quad (17)$$
$${}^{\bullet}OO-C(-R)-C(-R')-OH \rightleftarrows HOO-C(-R)-C(R')-O^{\bullet} \quad (18)$$
$$HOO-C(-R)-C(R')-O^{\bullet} \rightarrow R{-}C{=}O + R'{-}C{=}O + {}^{\bullet}OH \quad (19)$$

In this reaction sequence, the ˙OH radical which is involved in Reaction (16), is reformed through Reaction (19). Besides, the Korcek reaction mechanism [25-30] transforms γ-ketohydroperoxides into a carboxylic acid and a carbonyl. It can also participate to the oxidation of the fuel, as revealed by recent kinetic modeling and experimental works [31-33]. Lastly, other reaction routes, e.g., the formation of aromatic products through the CF oxidation of monoterpenes, have not been investigated in the literature.

In the present study, we aim to better characterize the autoxidation of three terpenes, i.e., limonene, α-pinene, and β-pinene (Fig. 2), under CF conditions and explore the formation of polyunsaturated and/or aromatics products. To attain these goals, we carried out oxidation experiments in a jet-stirred reactor at atmospheric pressure. The products of CF oxidation were characterized using soft ionization and high-resolution mass spectrometry. This study complements our previous works on terpenes oxidation [4, 5, 9] under CF conditions.

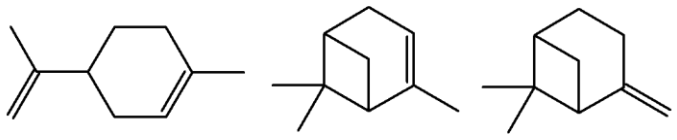

(a) (b) (c)

FIGURE 2: Chemical structure of the three terpenes, (a) limonene, (b) α-pinene, and (c) β-pinene, oxidized in this study.

2. MATERIALS AND METHODS

Oxidation experiments were carried out in a 42 mL fused silica jet-stirred-reactor (JSR) presented in previous papers [34, 35]. As in previous works [17, 22, 36], we injected the fuels in the JSR using a HPLC pump with online degasser. The fuels were delivered to an in-house vaporizer assembly fed with a flow of nitrogen. To avoid premature fuel oxidation, the fuel-N_2 (5.68:100 vol.) and O_2-N_2 (53.3:100 vol.) gas mixtures flowed

separately until they reach the JSR. Mass flow meters delivered the flow rates of nitrogen and oxygen. To verify the thermal homogeneity inside the JSR, a thermocouple (0.1 mm Pt-Pt/Rh-10% wires protected by a thin silica tube) was moved along the vertical axis of the reactor. Gradients of < 1 K/cm were recorded. The present experiments were conducted in the CF regime (520-680 K). 1 % of fuel was oxidized at 1 bar and a mean residence time of 1.5 s, in fuel-lean conditions ($\varphi = 0.5$).

To collect the products of oxidation, reacting mixtures were dissolved through bubbling into 250 mL of acetonitrile (≥ 99.9 pure, 273 K) for 90 min (Fig. 3). These samples were kept in a freezer at -15 °C for further analyses. Flow injection analyses with heated electrospray ionization (FIA/HESI) were carried out. This technique is well suited for analyzing species in the range 50-2000 Da. The liquid phase samples were analyzed using an Orbitrap Q-Exactive (high-resolution mass spectrometry, HRMS). We performed mass calibrations in positive and negative ionization modes using HESI calibration standards. We carried out reverse-phase ultra-high-performance liquid chromatography (RP-UHPLC) analyzes using a C18 analytical column (Phenomenex Luna, 1.6µm, 100 Å, 100x2.1 mm). The liquid samples (3 µL) were eluted by a water-acetonitrile (ACN) mix at a flow rate of 250 µL/min (gradient 5% to 90% ACN, during 33 min). We also used atmospheric pressure chemical ionization (APCI) in positive and negative modes. After RP-UHPLC separation, we determined the chemical structure of oxidation products by MS/MS analyses using the lowest collision cell energy (10 eV). As in previous works [17, 22, 36] we added 2,4-dinitrophenylhydrazine (2,4-DNPH) to liquid samples to assess the presence of carbonyl-containing compounds. As previously [17, 22, 36], we assessed the presence of hydroxyl (–OH) or hydroperoxy (–OOH) groups in the products by performing H/D exchange by adding D_2O to the liquid samples. The resulting solutions were analyzed by FIA-HESI-HRMS and RP-UHPLC-APCI-HRMS.

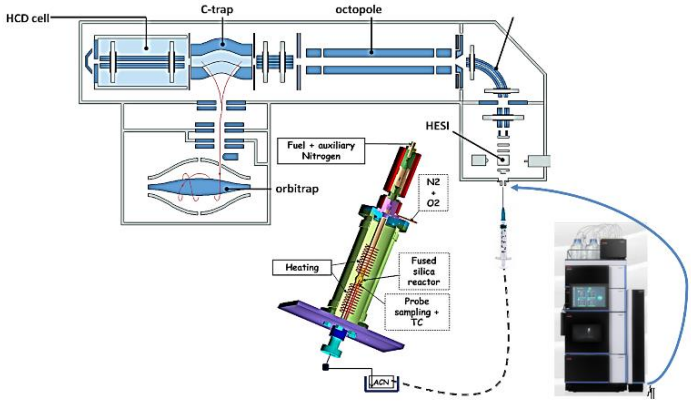

FIGURE 3: Schematic view of the experimental setup used: Orbitrap (top), JSR (middle), and UHPLC (right).

3. RESULTS AND DISCUSSION

Many products of CF oxidation were detected for the three terpenes. Oxidation products, containing ≥ 1 O-atom, were detected: $C_7H_{10}O_{4,5}$, $C_8H_{12}O_{2,4}$, $C_9H_{12}O$, $C_9H_{14}O_{1,3,5}$, $C_{10}H_{12}O_2$, $C_{10}H_{14}O_{1\text{-}9}$, $C_{10}H_{16}O_{2\text{-}5}$, and $C_{10}H_{18}O_6$. KHPs and their isomers have been characterized before by HRMS [4, 5, 9], and it was shown that the formation of these products peaks at a temperature ~ 620 K. Also, H/D exchange and reaction with 2,4-DNPH were used to assess the presence of OOH and C=O functional groups in the $C_{10}H_{14}O_3$ products, respectively. Carbonyl compounds formed through the Waddington mechanism on C=C double bonds of the fuels were observed as well as some of their oxidation products [4, 5, 9]. Among them, products of isoprenyl-6-oxo-heptanal ($C_{10}H_{16}O_2$), formed via the Waddington mechanism during limonene oxidation [4, 5, 9], were observed here. The oxidation of isoprenyl-6-oxo-heptanal can lead to the formation of three $C_{10}H_{14}O_2$ isomers. Several isomers were observed by UHPLC-HRMS (Fig. 4).

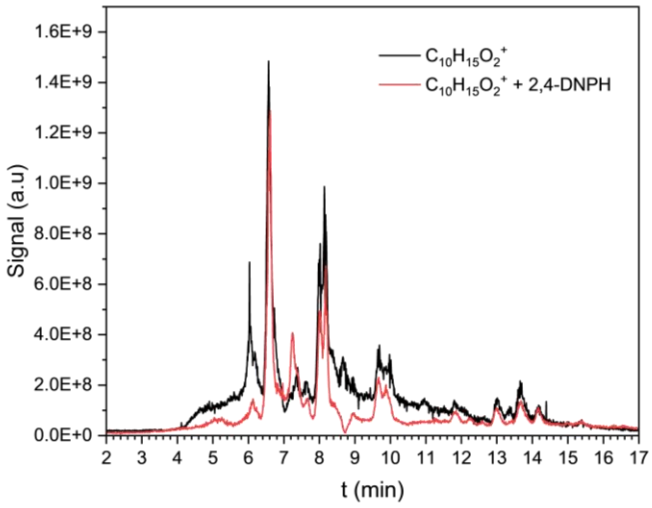

FIGURE 4: Chromatogram showing several isomers of $C_{10}H_{14}O_2$. After reaction with 2,4-DNPH, the signal recorded for products containing carbonyl groups decreases (red signal).

By calculating the dissociation energy of C-H bonds using the "BDE estimator" software [37], one can see that the isomer most likely to form is isomer A (Figure 5), due to the low dissociation energy of the C-Ha and C-Hb bonds.

Also using the BDE estimator, the dissociation energies of the C-H and C-C bonds of isomer A were calculated to obtain insights into the fragmentation mechanism that occurred in the collision cell (HCD) of the Orbitrap. The lowest bond dissociation energy corresponded to the bond between the carbon at position α with respect to the ketone function and that in α of the C=C group, i.e., BDE(C-C) = 69.8 kcal/mol. Dissociation of this bond in the HCD results in the formation of the $C_7H_9O^+$ ion fragment, which is one of the major fragments observed in the positive mode MS/MS spectrum of the isomer eluting at 6.62 min (Fig. 6).

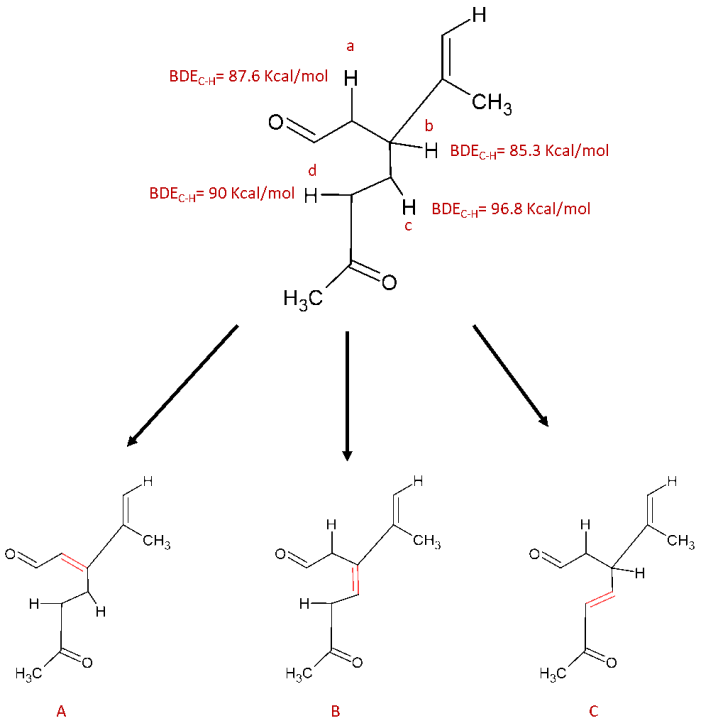

FIGURE 5: BDE in the isoprenyl-6-oxo-heptanal and possible decomposition products.

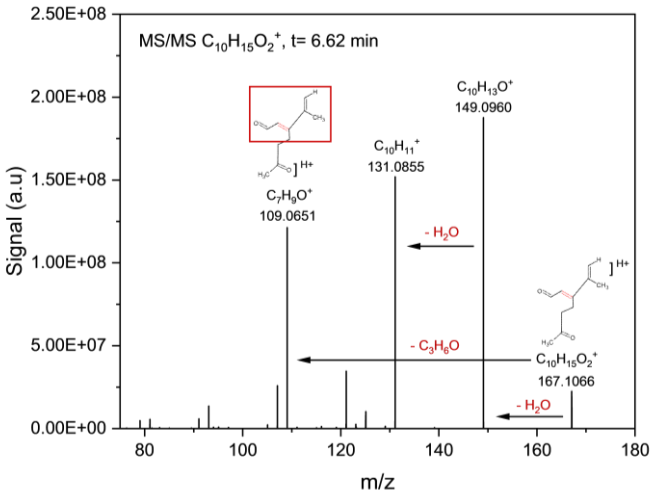

FIGURE 6: MS/MS spectrum in positive ionization mode of the $C_{10}H_{14}O_2$ isomer eluted at 6.62 min.

Furthermore, to confirm the presence of this species in our samples, the MS/MS spectrum in negative mode at a retention time of 6.62 min was studied. According to the calculations of the dissociation energies, the weakest C-H bond corresponds to the loss of the allylic hydrogen carried by the secondary carbon, i.e., BDE(C-H) = 83.8 kcal/mol. In this context, we estimated that, in APCI (–) mode, deprotonation occurs by the removal of this proton. As a result, we proposed a fragmentation mechanism for the $C_{10}H_{14}O_2$ isomer (A) deprotonated, as illustrated in Figure 7.

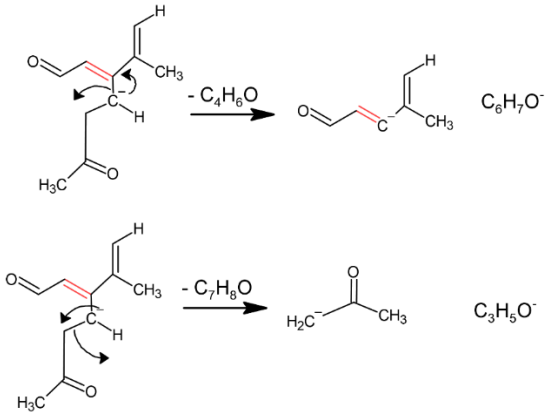

FIGURE 7: Fragmentation mechanism proposed for the deprotonated $C_{10}H_{14}O_2$ isomer (A).

The two fragments resulting from this mechanism are identical to those observed in the negative mode MS/MS spectrum of the $C_{10}H_{14}O_2$ isomer eluted at a retention time of 6.62 min (Fig. 8). This confirms the presence of this species in limonene oxidation products.

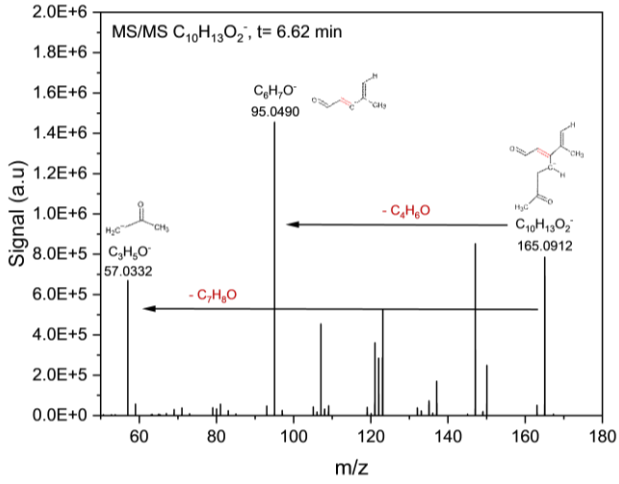

FIGURE 8: MS/MS spectrum in negative ionization mode of the $C_{10}H_{14}O_2$ isomer eluted at 6.62 min.

As mentioned in the Introduction, products of the Korcek mechanism are carboxylic acids and carbonyls. Such products were also detected in this work. Amongst the KHPs deriving from the oxidation of limonene, four could react via the Korcek mechanism. However, only one isomer can form a cyclic intermediate peroxide connecting the carbonyl and OOH groups to yield, via decomposition, a carbonyl product, $C_9H_{12}O$, and formic acid, CH_2O_2, (Fig. 9). In this work, both products were detected by UHPLC-HRMS. For the two other terpenes, products of the Korcek mechanism were also observed.

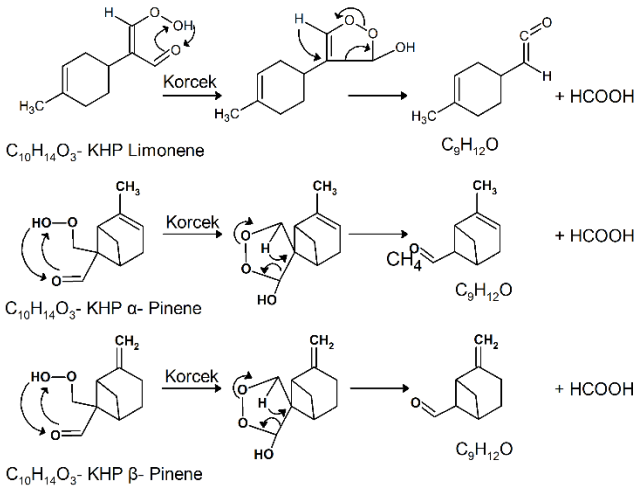

FIGURE 9: The Korcek mechanism participating to limonene, α-pinene, and β-pinene oxidation.

Combining HRMS with soft ionization (HESI, APCI) allows observing protonated and deprotonated ions through positive and negative modes of ionization, respectively. Very large datasets result from these analyses. Then a range of tools need to be used to identify chemical classes present in the samples, e.g., Van Krevelen plots (VK), Aromaticity index (AI), double bond equivalent (DBE), maximum carbonyl ratio (MCR), and Venn diagram. Such tools were used in the present study.

The VK diagrams can be used to identify different types of chemical compounds by combining the H/C and O/C ratios [38]. It is also possible to do a structural classification for each of these chemical compounds, for example by specifying the number of oxygen atoms, DBE, and AI. Recently, Zhang et al. [39] proposed a new index, the maximum carbonyl ration (MCR). It is defined as the ratio DBE/ number of O-atoms in chemical formulas, with DBE = 1 + C – H/2 (C and H represent the number of carbon and hydrogen atoms in chemical formulas, respectively). Depending on its value, this index breaks down the VK space into four chemical compound zones: 0<MCR<0.2 - very highly oxidized, 0.2-0.5 - highly oxidized, 0.5-0.9 - intermediately oxidized, 0.9-1 - oxidized unsaturated and highly unsaturated [40]. For chemical formulas with O/C = 0, we considered that MCR cannot be computed since these compounds are highly unsaturated and contain no carbonyl. The representation of the data obtained by (+/–) HESI-HRMS for the oxidation of the three terpenes in this space (Fig. 10) shows three boundaries. Chemical formulas found above line A contain between 0 and 20% C=O groups [39] whereas the rest is present in other functional groups, i.e., -OH, -OOH, ROR, ROOR. Chemical formulas found below line C would correspond to carbonylic oxygen [39]. In that region, one can observe chemical formulas with O/C = 0. Indeed, the formation of C_nH_2, C_nH_4, and C_nH_6 ($n \geq 4$) isomers was observed in VK plots for O/C = 0, using HESI+/– FIA-HRMS data (Fig. 10; the position of the fuels is shown as a circle). These plots indicated the formation of aromatic compounds (H/C < 0.8 and O/C = 0) and polyunsaturated compounds. In the area defined by 0 < O/C < 0.2 and H/C ≤ 1, we observed products resulting from oxidation and dehydrogenation processes.

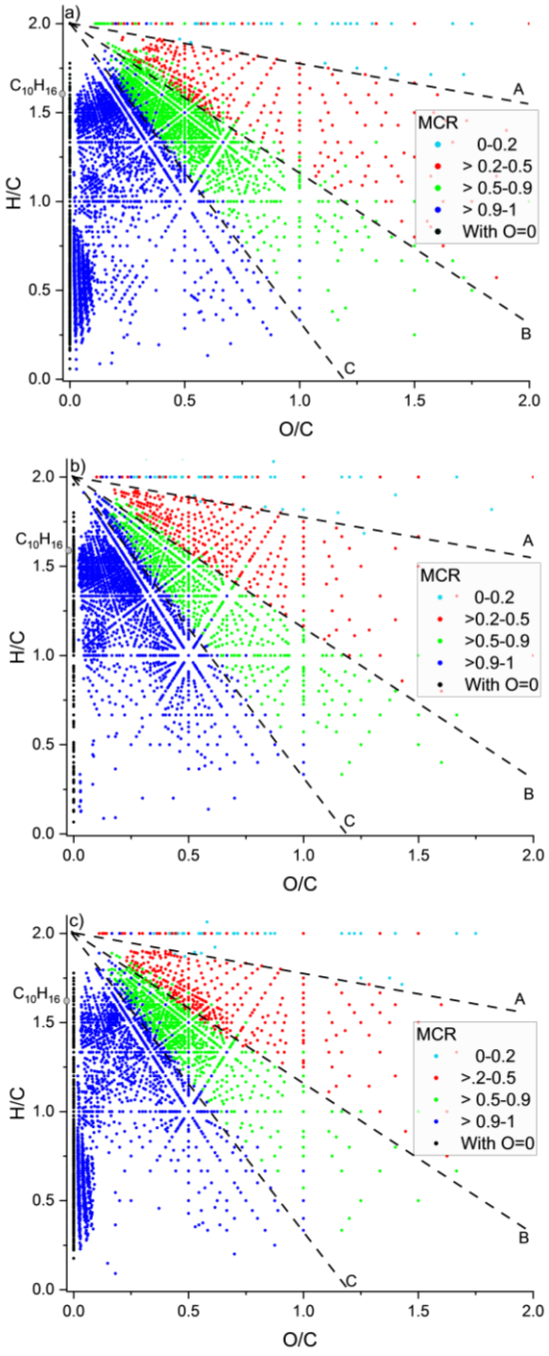

FIGURE 10: VK plots for the products of oxidation at 620 K of the 3 terpenes considered in this work (a: α-pinene, b: β-pinene, c: limonene). Color coding indicates the computed MCR in chemical formulas. The position of the fuel is shown as a circle on the O/C = 0 axis. $C_nH_mO_0$ compounds are shown as'●'.

The graphical similarities observed in VK space for these three terpenes were analyzed using a Venn diagram.

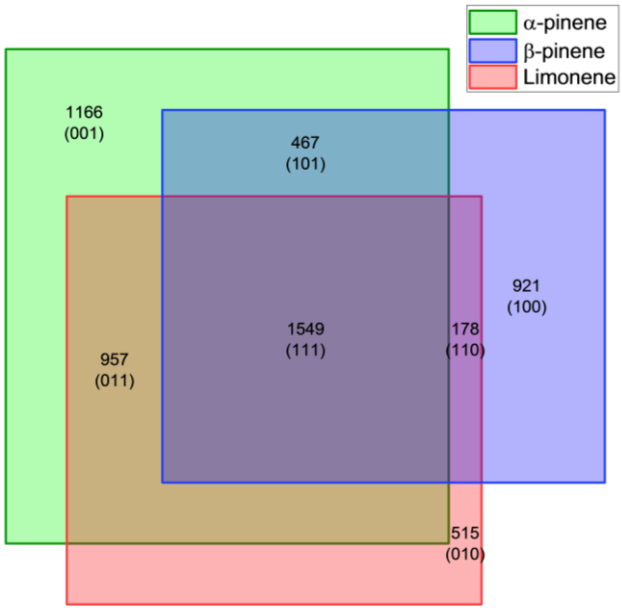

FIGURE 11: Venn diagram showing oxidation products common chemical formulas observed for the 3 fuels.

Figure 11 shows that 1549 common chemical formulas are found in the products of oxidation of the three fuels. Common chemical formulas are also observed for two fuels, whereas a large fraction of chemical formulas is found specifically for limonene, α-pinene, and β-pinene (515, 1166, and 921, respectively).

To better assess the presence of different chemical classes in oxidation products of limonene, α-pinene, and β-pinene, we computed the aromaticity index (AI = [1+C – O/2 – H/2] / [C – O/2]), where C, H, and O represent the number of carbon, hydrogen, and oxygen atoms, respectively, in the chemical formulas) [41, 42]. We defined chemical classes based on previous works [40]: aliphatic compounds (AI ≤ 0), olefinic products and naphthenic compounds (0 < AI ≤ 0.3) including the fuels which have an AI of 0.3, highly unsaturated compounds (0.3 < AI ≤ 0.5), aromatics (0.5 < AI ≤ 0.67), and polyaromatics (0.67 < AI). As can be seen from Figure 12, for limonene, α-pinene, and β-pinene a significant fraction of aromatics and polyaromatics is present in the oxidation products. They are also shown in VK plots for H/C ≤ 0.8 and O/C = 0. When we examine the common dataset composed of 1549 chemical formulas, the relative importance of the 5 chemical classes is rather similar, even for aromatics and polyaromatics (Fig 12 (d)).

The present work has demonstrated the complexity of terpenes oxidation chemistry under cool flame conditions. Whereas many products of oxidation were observed, their quantification needs to be addressed in future work. Such quantitative data would be of great importance for proposing kinetic reaction mechanism usable for modeling combustion in engines.

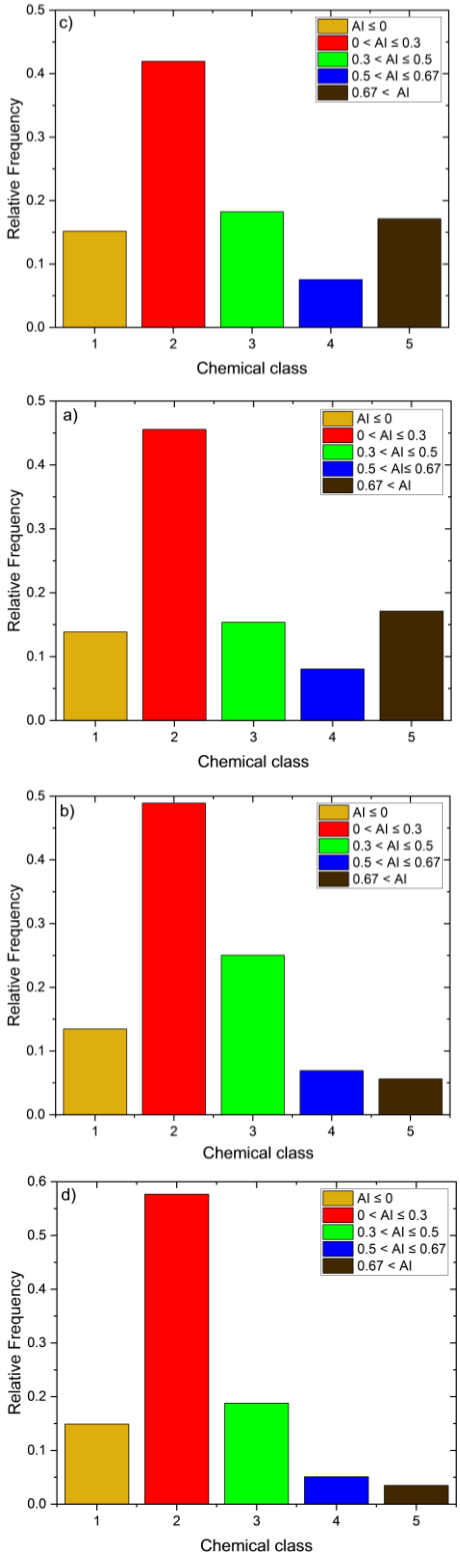

FIGURE 12: Chemical classes found in the oxidation products of (a) α-pinene, (b) β-pinene, (c) limonene, and (d) for the 1549 chemical formulas common to (a), (b), and (c).

4. CONCLUSION

Limonene, α-pinene, and β-pinene were oxidized in a JSR at 1 bar, in the cool flame regime. A large set of chemical formulas was observed, including highly oxygenated products. High-resolution mass spectrometry combined with graphic tools were used to demonstrate the formation of aromatic and/or polyunsaturated and highly oxygenated products.

ACKNOWLEDGEMENTS

Support from the CAPRYSSES project (ANR- 11-LABX-006–01) funded by ANR through the PIA (Programme d'Investissement d'Avenir) is gratefully acknowledged. ZD thanks the French Ministry of Research and Higher Education (MESR) for a PhD grant.

REFERENCES

[1] Seinfeld, J. H., and Pandis, S. N., Atmospheric Chemistry and Physics: From Air Pollution to Climate Change, *Wiley-Interscience*, Hoboken, NJ, 2006.

[2] Pourbafrani, M., Forgács, G., Horváth, I. S., Niklasson, C., and Taherzadeh, M. J., Production of Biofuels, Limonene and Pectin from Citrus Wastes, *Bioresource Technology*, 101(11) (2010) 4246-4250.

[3] Mewalal, R., Rai, D. K., Kainer, D., Chen, F., Külheim, C., Peter, G. F., and Tuskan, G. A., Plant-Derived Terpenes: A Feedstock for Specialty Biofuels, *Trends in Biotechnology*, 35(3) (2017) 227-240.

[4] Benoit, R., Belhadj, N., Lailliau, M., and Dagaut, P., On the Similarities and Differences between the Products of Oxidation of Hydrocarbons under Simulated Atmospheric Conditions and Cool Flames, *Atmospheric Chemistry and Physics*, 21(10) (2021) 7845-7862.

[5] Benoit, R., Belhadj, N., Dbouk, Z., Lailliau, M., and Dagaut, P., On the Formation of Highly Oxidized Pollutants by Autoxidation of Terpenes under Low-Temperature-Combustion Conditions: The Case of Limonene and A-Pinene, *Atmos. Chem. Phys.*, 23(10) (2023) 5715-5733.

[6] Vereecken, L., and Peeters, J., Nontraditional (Per)Oxy Ring-Closure Paths in the Atmospheric Oxidation of Isoprene and Monoterpenes, *Journal of Physical Chemistry A*, 108(24) (2004) 5197-5204.

[7] Witkowski, B., and Gierczak, T., Characterization of the Limonene Oxidation Products with Liquid Chromatography Coupled to the Tandem Mass Spectrometry, *Atmospheric Environment*, 154((2017) 297-307.

[8] Piletic, I. R., and Kleindienst, T. E., Rates and Yields of Unimolecular Reactions Producing Highly Oxidized Peroxy Radicals in the Oh-Induced Autoxidation of Alpha-Pinene, Beta-Pinene, and Limonene, *Journal of Physical Chemistry A*, 126(1) (2022) 88-100.

[9] Dbouk, Z., Belhadj, N., Lailliau, M., Benoit, R., and Dagaut, P., Characterization of the Autoxidation of Terpenes at Elevated Temperature Using High-Resolution Mass Spectrometry: Formation of Ketohydroperoxides and Highly Oxidized Products from Limonene, *Journal of Physical Chemistry A*, 126(48) (2022) 9087-9096.

[10] Courty, L., Chetehouna, K., Halter, F., Foucher, F., Garo, J. P., and Mounaim-Rousselle, C., Experimental Determination of Emission and Laminar Burning Speeds of Alpha-Pinene, *Combustion and Flame*, 159(4) (2012) 1385-1392.

[11] Chetehouna, K., Courty, L., Mounaim-Rousselle, C., Halter, F., and Garo, J.-P., Combustion Characteristics of P-Cymene Possibly Involved in Accelerating Forest Fires, *Combustion Science and Technology*, 185(9) (2013) 1295-1305.

[12] Courty, L., Chetehouna, K., Chen, Z., Halter, F., Mounaim-Rousselle, C., and Garo, J.-P., Determination of Laminar Burning Speeds and Markstein Lengths of P-Cymene/Air Mixtures Using Three Models, *Combustion Science and Technology*, 186(4-5) (2014) 490-503.

[13] Bierkandt, T., Hoener, M., Gaiser, N., Hansen, N., Koehler, M., and Kasper, T., Experimental Flat Flame Study of Monoterpenes: Insights into the Combustion Kinetics of Alpha-Pinene, Beta-Pinene, and Myrcene, *Proceedings of the Combustion Institute*, 38(2) (2021) 2431-2440.

[14] Mack, J. H., Rapp, V. H., Broeckelmann, M., Lee, T. S., and Dibble, R. W., Investigation of Biofuels from Microorganism Metabolism for Use as Anti-Knock Additives, *Fuel*, 117((2014) 939-943.

[15] Morley, C., A Fundamentally Based Correlation between Alkane Structure and Octane Number, *Combustion Science and Technology*, 55(4-6) (1987) 115-123.

[16] Benson, S. W., The Kinetics and Thermochemistry of Chemical Oxidation with Application to Combustion and Flames, *Progress in Energy and Combustion Science*, 7(2) (1981) 125-134.

[17] Belhadj, N., Benoit, R., Dagaut, P., and Lailliau, M., Experimental Characterization of Tetrahydrofuran Low-Temperature Oxidation Products Including Ketohydroperoxides and Highly Oxygenated Molecules, *Energy & Fuels*, 35(9) (2021) 7242–7252.

[18] Belhadj, N., Benoit, R., Dagaut, P., Lailliau, M., Serinyel, Z., Dayma, G., Khaled, F., Moreau, B., and Foucher, F., Oxidation of Di-N-Butyl Ether: Experimental Characterization of Low-Temperature Products in Jsr and Rcm, *Combustion and Flame*, 222((2020) 133-144.

[19] Wang, Z., Popolan-Vaida, D. M., Chen, B., Moshammer, K., Mohamed, S. Y., Wang, H., Sioud, S., Raji, M. A., Kohse-Höinghaus, K., Hansen, N., Dagaut, P., Leone, S. R., and Sarathy, S. M., Unraveling the Structure and Chemical Mechanisms of Highly Oxygenated Intermediates in Oxidation of Organic Compounds, *Proceedings of the National Academy of Sciences*, 114(50) (2017) 13102-13107.

[20] Wang, Z. D., Chen, B. J., Moshammer, K., Popolan-Vaida, D. M., Sioud, S., Shankar, V. S. B., Vuilleumier, D., Tao, T., Ruwe, L., Brauer, E., Hansen, N., Dagaut, P., Kohse-Hoinghaus, K., Raji, M. A., and Sarathy, S. M., N-Heptane Cool Flame Chemistry: Unraveling Intermediate Species Measured in a Stirred Reactor and Motored Engine, *Combustion and Flame*, 187((2018) 199-216.

[21] Belhadj, N., Lailliau, M., Benoit, R., and Dagaut, P., Experimental and Kinetic Modeling Study of N-Hexane

Oxidation. Detection of Complex Low-Temperature Products Using High-Resolution Mass Spectrometry, *Combustion and Flame*, 233((2021) 111581.

[22] Belhadj, N., Lailliau, M., Benoit, R., and Dagaut, P., Towards a Comprehensive Characterization of the Low-Temperature Autoxidation of Di-N-Butyl Ether, *Molecules*, 26(23) (2021) 7174.

[23] Liu, B. Z., Di, Q. M., Lailliau, M., Belhadj, N., Dagaut, P., and Wang, Z. D., Experimental and Kinetic Modeling Study of Low-Temperature Oxidation of N -Pentane, *Combustion and Flame*, 254((2023) 12813-12813.

[24] Ray, D. J. M., Redfearn, A., and Waddington, D. J., Gas-Phase Oxidation of Alkenes: Decomposition of Hydroxy-Substituted Peroxyl Radicals, *Journal of the Chemical Society, Perkin Transactions 2*, 5) (1973) 540-543.

[25] Jalan, A., Alecu, I. M., Meana-Paneda, R., Aguilera-Iparraguirre, J., Yang, K. R., Merchant, S. S., Truhlar, D. G., and Green, W. H., New Pathways for Formation of Acids and Carbonyl Products in Low-Temperature Oxidation: The Korcek Decomposition of Gamma-Ketohydroperoxides, *Journal of the American Chemical Society*, 135(30) (2013) 11100-11114.

[26] Jensen, R. K., Korcek, S., Mahoney, L. R., and Zinbo, M., Liquid-Phase Autoxidation of Organic-Compounds at Elevated-Temperatures .1. Stirred Flow Reactor Technique and Analysis of Primary Products from Normal-Hexadecane Autoxidation at 120-Degrees-C 180-Degrees-C, *Journal of the American Chemical Society*, 101(25) (1979) 7574-7584.

[27] Jensen, R. K., Korcek, S., Mahoney, L. R., and Zinbo, M., Liquid-Phase Autoxidation of Organic-Compounds at Elevated-Temperatures .2. Kinetics and Mechanisms of the Formation of Cleavage Products in Normal-Hexadecane Autoxidation, *Journal of the American Chemical Society*, 103(7) (1981) 1742-1749.

[28] Jensen, R. K., Zinbo, M., and Korcek, S., Hplc Determination of Hydroperoxidic Products Formed in the Autoxidation of Normal-Hexadecane at Elevated-Temperatures, *Journal of Chromatographic Science*, 21(9) (1983) 394-397.

[29] Jensen, R. K., Korcek, S., Zinbo, M., and Johnson, M. D., Initiation in Hydrocarbon Autoxidation at Elevated-Temperatures, *International Journal of Chemical Kinetics*, 22(10) (1990) 1095-1107.

[30] Jensen, R. K., Korcek, S., and Zinbo, M., Formation, Isomerization, and Cyclization Reactions of Hydroperoxyalkyl Radicals in Hexadecane Autoxidation at 160-190-Degrees-C, *Journal of the American Chemical Society*, 114(20) (1992) 7742-7748.

[31] Popolan-Vaida, D. M., Eskola, A. J., Rotavera, B., Lockyear, J. F., Wang, Z. D., Sarathy, S. M., Caravan, R. L., Zador, J., Sheps, L., Lucassen, A., Moshammer, K., Dagaut, P., Osborn, D. L., Hansen, N., Leone, S. R., and Taatjes, C. A., Formation of Organic Acids and Carbonyl Compounds in N-Butane Oxidation Via Gamma-Ketohydroperoxide Decomposition, *Angewandte Chemie-International Edition*, 61(42) (2022) 9168-9168.

[32] Ranzi, E., Cavallotti, C., Cuoci, A., Frassoldati, A., Pelucchi, M., and Faravelli, T., New Reaction Classes in the Kinetic Modeling of Low Temperature Oxidation of N-Alkanes, *Combustion and Flame*, 162(5) (2015) 1679-1691.

[33] Xie, C., Lailliau, M., Issayev, G., Xu, Q., Chen, W., Dagaut, P., Farooq, A., Sarathy, S. M., Wei, L., and Wang, Z., Revisiting Low Temperature Oxidation Chemistry of N-Heptane, *Combustion and Flame*, 242((2022) 112177.

[34] Dagaut, P., Cathonnet, M., Rouan, J. P., Foulatier, R., Quilgars, A., Boettner, J. C., Gaillard, F., and James, H., A Jet-Stirred Reactor for Kinetic Studies of Homogeneous Gas-Phase Reactions at Pressures up to Ten Atmospheres (≈1 Mpa), *Journal of Physics E: Scientific Instruments*, 19(3) (1986) 207-209.

[35] Dagaut, P., Cathonnet, M., and Boettner, J. C., Experimental-Study and Kinetic Modeling of Propene Oxidation in a Jet Stirred Flow Reactor, *Journal of Physical Chemistry*, 92(3) (1988) 661-671.

[36] Belhadj, N., Lailliau, M., Dbouk, Z., Benoit, R., Moreau, B., Foucher, F., and Dagaut, P., Gasoline Surrogate Oxidation in a Motored Engine, a Jsr, and an Rcm: Characterization of Cool-Flame Products by High-Resolution Mass Spectrometry, *Energy & Fuels*, 36(7) (2022) 3893-3908.

[37] St. John, P. C., Guan, Y., Kim, Y., Kim, S., and Paton, R. S., Prediction of Organic Homolytic Bond Dissociation Enthalpies at near Chemical Accuracy with Sub-Second Computational Cost, *Nature Communications*, 11(1) (2020) 2328.

[38] D'andrilli, J., Cooper, W. T., Foreman, C. M., and Marshall, A. G., An Ultrahigh-Resolution Mass Spectrometry Index to Estimate Natural Organic Matter Lability, *Rapid Communications in Mass Spectrometry*, 29(24) (2015) 2385-2401.

[39] Zhang, Y., Wang, K., Tong, H., Huang, R.-J., and Hoffmann, T., The Maximum Carbonyl Ratio (Mcr) as a New Index for the Structural Classification of Secondary Organic Aerosol Components, *Rapid Communications in Mass Spectrometry*, 35(14) (2021) e9113.

[40] Schneider, E., Czech, H., Popovicheva, O., Chichaeva, M., Kobelev, V., Kasimov, N., Minkina, T., Rüger, C. P., and Zimmermann, R., Comprehensive Mass Spectrometric Analysis of Unprecedented High Levels of Carbonaceous Aerosol Particles Long-Range Transported from Wildfires in the Siberian Arctic, *EGUsphere*, 2023((2023) 1-33.

[41] Brege, M. A., China, S., Schum, S., Zelenyuk, A., and Mazzoleni, L. R., Extreme Molecular Complexity Resulting in a Continuum of Carbonaceous Species in Biomass Burning Tar Balls from Wildfire Smoke, *ACS Earth and Space Chemistry*, 5(10) (2021) 2729-2739.

[42] Koch, B. P., and Dittmar, T., From Mass to Structure: An Aromaticity Index for High-Resolution Mass Data of Natural Organic Matter, *Rapid Communications in Mass Spectrometry*, 30(1) (2016) 250-250.